

Three-nucleon force at large distances: Insights from chiral effective field theory and the large- N_c expansion

E. Epelbaum,^{1,*} A. M. Gasparyan,^{1,2,†} H. Krebs,^{1,‡} and C. Schat^{3,§}

¹*Institut für Theoretische Physik II, Ruhr-Universität Bochum, D-44780 Bochum, Germany*

²*SSC RF ITEP, Bolshaya Cheremushkinskaya 25, 117218 Moscow, Russia*

³*Departamento de Física, FCEyN, Universidad de Buenos Aires and IFIBA, CONICET, Ciudad Universitaria, Pab. 1, (1428) Buenos Aires, Argentina*

(Dated: November 14, 2014)

We confirm the claim of Ref. [1] that 20 operators are sufficient to represent the most general local isospin-invariant three-nucleon force and derive explicit relations between the two sets of operators suggested in Refs. [1] and [2]. We use the set of 20 operators to discuss the chiral expansion of the long- and intermediate-range parts of the three-nucleon force up to next-to-next-to-next-to-next-to-leading order in the standard formulation without explicit $\Delta(1232)$ degrees of freedom. We also address implications of the large- N_c expansion in QCD for the size of the various three-nucleon force contributions.

PACS numbers: 13.75.Cs, 21.30.-x

I. INTRODUCTION

The three-nucleon force (3NF) has been a subject of intense research in nuclear physics for many decades, see Refs. [3, 4] for recent review articles. Explicit calculations have demonstrated that 3NFs have significant effects in spectra and other properties of light and medium-mass nuclei, see Refs. [5–10] for a selection of recent studies along these lines. Three-body continuum provides an even more clean and detailed testing ground for 3NFs. In particular, one expects that 3NF will resolve several puzzles observed in nucleon-deuteron (Nd) scattering at low energy such as the underprediction of the vector analyzing power in elastic Nd scattering known as the A_y puzzle and the discrepancy observed for the cross section in the so-called symmetric space star configuration of the deuteron break up, see [3] and references therein. Moreover, effects of the 3NF in Nd scattering are expected to become more prominent at energies above $E_{\text{lab}} \sim 100$ MeV, where large deviations between calculations based on modern high-precision potential models and experimental data are observed [11]. The currently available phenomenological 3NF models are unable to explain these differences in elastic scattering and deuteron breakup reactions which especially applies to spin-dependent observables [3]. The much worse understanding of the spin structure of the 3NF compared to the two-nucleon force is, to a large extent, due to a much richer operator structure of the 3NF, a large computational effort needed to solve the three-body Faddeev equations and a considerably more scarce data base in the three-nucleon sector. Further progress in this field clearly requires guidance from the theory in form of lattice QCD [12], chiral effective field theory (EFT) [13] or large- N_c expansion in QCD [1].

In the present work, we mainly focus on the description of the 3NF within the chiral expansion. Chiral EFT provides a systematic and model independent approach to nuclear forces which relies on the symmetries of QCD such as especially the spontaneously broken approximate chiral symmetry, see Ref. [14] for an introduction and Refs. [13, 15] for recent review articles on this subject. The first nonvanishing contributions to the 3NF appear at next-to-next-to-leading order ($N^2\text{LO}$) in the chiral expansion [16]¹ and are given by tree-level diagrams representing two-pion (2π) exchange, one-pion exchange-contact and purely short-range contact interactions. The resulting 3NF at $N^2\text{LO}$ has

*Email: evgeny.epelbaum@rub.de

†Email: ashot.gasparyan@rub.de

‡Email: hermann.krebs@rub.de

§Email: carlos.schat@gmail.com

¹ This statement applies to energy-independent formulations of nuclear potentials.

been extensively explored in few- and many-body studies during the past decade. Leading corrections to the 3NF emerge at next-to-next-to-leading order (N³LO) from one-loop diagrams constructed from the lowest-order vertices in the effective Lagrangian and have been worked out recently [17–19]. The very first calculations of nucleon-deuteron scattering observables using the 3NF up to N³LO indicate that the N³LO corrections are rather weak and will not provide solution to the low-energy puzzles mentioned above [20, 21]. In fact, given that the lowest-order pion-nucleon vertices in the effective chiral Lagrangian do *not* receive contributions from the $\Delta(1232)$ resonance, one might expect large corrections from subleading, i.e. next-to-next-to-next-to-next-to-leading order (N⁴LO) terms. The corresponding long- and intermediate-range contributions are driven by the low-energy constants (LECs) c_i which accompany subleading pion-nucleon vertices. The LECs $c_{2,3,4}$ are, to a large extent, governed by the Δ isobar and known to be numerically rather large. This observation provides a strong motivation to extend the derivation of the 3NF to N⁴LO in the chiral expansion. In Refs. [2, 22], this task was accomplished for the longest-range 2π -exchange and the intermediate-range two-pion-one-pion (2π - 1π) exchange and ring topologies, respectively. In order to be able to address the convergence of the chiral expansion in a meaningful way, a set of 22 operators parametrizing the most general operator structure of a local 3NF was suggested in Ref. [2]. By applying all possible permutations of the nucleon labels, these operators give rise to 89 structures in the 3NF. The structure of the 3NF was also analyzed independently in Ref. [1] in the context of the large- N_c expansion in QCD. It was found in this work that only 80 independent structures appear in a most general parametrization of a local 3NF.

In this paper we confirm the conclusion of Ref. [1] that the number of independent operators for the local three-nucleon force can be reduced to 80 and give a set of 20 operators which generate these 80 structures upon performing all possible permutations. Since these findings affect the results for the structure functions in coordinate space plotted in Figs. 4-8 of Ref. [2], we re-analyze the chiral expansion of the long- and intermediate-range topologies employing the new set of 20 operators. We also correct for a numerical error we found in the Fourier transformation of the 2π -exchange in Ref. [2] which resulted in enhanced size of certain structure functions. Notice that only figures but none of the expressions given in that work are affected by the above-mentioned error. Finally, we discuss implications of the large- N_c expansion in QCD for the size of the various three-nucleon force contributions.

Our paper is organized as follows. In section II we provide explicit relations between the redundant operators given in Ref. [2] and define a set of 20 independent operators both in coordinate and momentum spaces. Next, in section III, we show the results for the corresponding structure functions of the 2π -, 2π - 1π -exchange and ring topologies in the equilateral triangle configuration and discuss convergence of the chiral expansion. Section IV addresses implications of the large- N_c expansion on the size of the various terms. Finally, the main results of this study are summarized in section V.

II. LOCAL THREE-NUCLEON FORCES

A general local three-nucleon force in momentum space can be written in a form

$$V_{3N} = \sum_i O_i(\vec{\sigma}_1, \vec{\sigma}_2, \vec{\sigma}_3, \boldsymbol{\tau}_1, \boldsymbol{\tau}_2, \boldsymbol{\tau}_3, \vec{q}_1, \vec{q}_3) F_i(q_1, q_3, \vec{q}_1 \cdot \vec{q}_3),$$

where $\vec{\sigma}_i$ ($\boldsymbol{\tau}_i$) denote spin (isospin) Pauli matrices for the nucleon i and $\vec{q}_i = \vec{p}_i' - \vec{p}_i$, with \vec{p}_i' and \vec{p}_i being the final and initial momenta of the nucleon i . Further, O_i are spin-momentum-isospin operators and the scalar structure functions F_i depend on $q_1 \equiv |\vec{q}_1|$, $q_3 \equiv |\vec{q}_3|$ and the scalar product $\vec{q}_1 \cdot \vec{q}_3$ or, equivalently, on q_1 , q_2 and q_3 . Here and in the following, we require that the 3NF V_{3N} is given in a symmetrized form with respect to interchanging the nucleon labels. Assuming parity and time-reversal invariance as well as isospin symmetry, a set of 89 operators O_i was suggested in Ref. [2]. Alternatively, V_{3N} can be generated by 22 operators upon applying all possible permutations of the nucleon labels

$$V_{3N} = \sum_{i=1}^{22} \mathcal{G}_i(\vec{\sigma}_1, \vec{\sigma}_2, \vec{\sigma}_3, \boldsymbol{\tau}_1, \boldsymbol{\tau}_2, \boldsymbol{\tau}_3, \vec{q}_1, \vec{q}_3) \mathcal{F}_i(q_1, q_3, \vec{q}_1 \cdot \vec{q}_3) + 5 \text{ permutations}, \quad (2.1)$$

where \mathcal{F}_i denote the structure functions in this representation. We show in Table I both sets of the operators given in Ref. [2]. The functions $S, A, G_{11}, G_{12}, G_{21}, G_{22}$ appearing in this table refer to the corresponding irreducible representations of the group S_3 and are defined via:

$$S(O) = \frac{1}{6} \sum_{P \in S_3} PO, \quad A(O) = \frac{1}{6} \sum_{P \in S_3} (-1)^{w(P)} PO, \quad G_{ij}(O) = \frac{1}{3} \sum_{P \in S_3} \mathcal{D}_{ij}(P) PO, \quad \text{with } i, j = 1, 2, \quad (2.2)$$

Generators \mathcal{G} of 89 independent operators	S	A	G_{12}	G_{22}	G_{11}	G_{21}
$\mathcal{G}_1 = 1$	O_1	0	0	0	0	0
$\mathcal{G}_2 = \boldsymbol{\tau}_1 \cdot \boldsymbol{\tau}_3$	O_2	0	O_3	O_4	0	0
$\mathcal{G}_3 = \vec{\sigma}_1 \cdot \vec{\sigma}_3$	O_5	0	O_6	O_7	0	0
$\mathcal{G}_4 = \boldsymbol{\tau}_1 \cdot \boldsymbol{\tau}_3 \vec{\sigma}_1 \cdot \vec{\sigma}_3$	O_8	0	O_9	O_{10}	0	0
$\mathcal{G}_5 = \boldsymbol{\tau}_2 \cdot \boldsymbol{\tau}_3 \vec{\sigma}_1 \cdot \vec{\sigma}_2$	O_{11}	O_{12}	O_{13}	O_{14}	O_{15}	O_{16}
$\mathcal{G}_6 = \boldsymbol{\tau}_1 \cdot (\boldsymbol{\tau}_2 \times \boldsymbol{\tau}_3) \vec{\sigma}_1 \cdot (\vec{\sigma}_2 \times \vec{\sigma}_3)$	O_{17}	0	0	0	0	0
$\mathcal{G}_7 = \boldsymbol{\tau}_1 \cdot (\boldsymbol{\tau}_2 \times \boldsymbol{\tau}_3) \vec{\sigma}_2 \cdot (\vec{q}_1 \times \vec{q}_3)$	O_{18}	0	O_{19}	O_{20}	0	0
$\mathcal{G}_8 = \vec{q}_1 \cdot \vec{\sigma}_1 \vec{q}_1 \cdot \vec{\sigma}_3$	O_{21}	O_{22}	O_{23}	O_{24}	O_{25}	O_{26}
$\mathcal{G}_9 = \vec{q}_1 \cdot \vec{\sigma}_3 \vec{q}_3 \cdot \vec{\sigma}_1$	O_{27}	0	O_{28}	O_{29}	0	0
$\mathcal{G}_{10} = \vec{q}_1 \cdot \vec{\sigma}_1 \vec{q}_3 \cdot \vec{\sigma}_3$	O_{30}	0	O_{31}	O_{32}	0	0
$\mathcal{G}_{11} = \boldsymbol{\tau}_2 \cdot \boldsymbol{\tau}_3 \vec{q}_1 \cdot \vec{\sigma}_1 \vec{q}_1 \cdot \vec{\sigma}_2$	O_{33}	O_{34}	O_{35}	O_{36}	O_{37}	O_{38}
$\mathcal{G}_{12} = \boldsymbol{\tau}_2 \cdot \boldsymbol{\tau}_3 \vec{q}_1 \cdot \vec{\sigma}_1 \vec{q}_3 \cdot \vec{\sigma}_2$	O_{39}	O_{40}	O_{41}	O_{42}	O_{43}	O_{44}
$\mathcal{G}_{13} = \boldsymbol{\tau}_2 \cdot \boldsymbol{\tau}_3 \vec{q}_3 \cdot \vec{\sigma}_1 \vec{q}_1 \cdot \vec{\sigma}_2$	O_{45}	O_{46}	O_{47}	O_{48}	O_{49}	O_{50}
$\mathcal{G}_{14} = \boldsymbol{\tau}_2 \cdot \boldsymbol{\tau}_3 \vec{q}_3 \cdot \vec{\sigma}_1 \vec{q}_3 \cdot \vec{\sigma}_2$	O_{51}	O_{52}	O_{53}	O_{54}	O_{55}	O_{56}
$\mathcal{G}_{15} = \boldsymbol{\tau}_1 \cdot \boldsymbol{\tau}_3 \vec{q}_2 \cdot \vec{\sigma}_1 \vec{q}_2 \cdot \vec{\sigma}_3$	O_{57}	0	O_{58}	O_{59}	0	0
$\mathcal{G}_{16} = \boldsymbol{\tau}_2 \cdot \boldsymbol{\tau}_3 \vec{q}_3 \cdot \vec{\sigma}_2 \vec{q}_3 \cdot \vec{\sigma}_3$	O_{60}	O_{61}	O_{62}	O_{63}	O_{64}	O_{65}
$\mathcal{G}_{17} = \boldsymbol{\tau}_1 \cdot \boldsymbol{\tau}_3 \vec{q}_1 \cdot \vec{\sigma}_1 \vec{q}_3 \cdot \vec{\sigma}_3$	O_{66}	0	O_{67}	O_{68}	0	0
$\mathcal{G}_{18} = \boldsymbol{\tau}_1 \cdot (\boldsymbol{\tau}_2 \times \boldsymbol{\tau}_3) \vec{\sigma}_1 \cdot \vec{\sigma}_3 \vec{\sigma}_2 \cdot (\vec{q}_1 \times \vec{q}_3)$	O_{69}	0	O_{70}	O_{71}	0	0
$\mathcal{G}_{19} = \boldsymbol{\tau}_1 \cdot (\boldsymbol{\tau}_2 \times \boldsymbol{\tau}_3) \vec{\sigma}_3 \cdot \vec{q}_1 \vec{q}_1 \cdot (\vec{\sigma}_1 \times \vec{\sigma}_2)$	O_{72}	O_{73}	O_{74}	O_{75}	O_{76}	O_{77}
$\mathcal{G}_{20} = \boldsymbol{\tau}_1 \cdot (\boldsymbol{\tau}_2 \times \boldsymbol{\tau}_3) \vec{\sigma}_1 \cdot \vec{q}_1 \vec{\sigma}_2 \cdot \vec{q}_1 \vec{\sigma}_3 \cdot (\vec{q}_1 \times \vec{q}_3)$	O_{78}	O_{79}	O_{80}	O_{81}	O_{82}	O_{83}
$\mathcal{G}_{21} = \boldsymbol{\tau}_1 \cdot (\boldsymbol{\tau}_2 \times \boldsymbol{\tau}_3) \vec{\sigma}_1 \cdot \vec{q}_2 \vec{\sigma}_3 \cdot \vec{q}_2 \vec{\sigma}_2 \cdot (\vec{q}_1 \times \vec{q}_3)$	O_{84}	0	O_{85}	O_{86}	0	0
$\mathcal{G}_{22} = \boldsymbol{\tau}_1 \cdot (\boldsymbol{\tau}_2 \times \boldsymbol{\tau}_3) \vec{\sigma}_1 \cdot \vec{q}_1 \vec{\sigma}_3 \cdot \vec{q}_3 \vec{\sigma}_2 \cdot (\vec{q}_1 \times \vec{q}_3)$	O_{87}	0	O_{88}	O_{89}	0	0

TABLE I: The set of 22 generating operators \mathcal{G}_i and their relation to 89 operators O_1, \dots, O_{89} suggested in Ref. [2]. The operators O_i are generated by application of one of the 6 functions $S, A, G_{11}, G_{12}, G_{21}, G_{22}$ defined in the text on the corresponding operator \mathcal{G}_j .

where $w(P) = \pm 1$ for even/odd permutations and the matrices \mathcal{D} for the two-dimensional representation can be chosen e.g. in the form

$$\begin{aligned}
\mathcal{D}((1)) &= \begin{pmatrix} 1 & 0 \\ 0 & 1 \end{pmatrix}, & \mathcal{D}((12)) &= \frac{1}{2} \begin{pmatrix} 1 & \sqrt{3} \\ \sqrt{3} & -1 \end{pmatrix}, & \mathcal{D}((13)) &= \begin{pmatrix} -1 & 0 \\ 0 & 1 \end{pmatrix}, \\
\mathcal{D}((23)) &= -\frac{1}{2} \begin{pmatrix} -1 & \sqrt{3} \\ \sqrt{3} & 1 \end{pmatrix}, & \mathcal{D}((123)) &= -\frac{1}{2} \begin{pmatrix} 1 & \sqrt{3} \\ -\sqrt{3} & 1 \end{pmatrix}, & \mathcal{D}((132)) &= -\frac{1}{2} \begin{pmatrix} 1 & -\sqrt{3} \\ \sqrt{3} & 1 \end{pmatrix},
\end{aligned} \tag{2.3}$$

see Ref. [2] for more details.

As pointed out in Ref. [1], the number of independent operators for the local three-nucleon force can be reduced from 89 to 80. This can be most easily seen by forming irreducible tensor operators separately from the Pauli matrices and momenta and contracting them with each other. More precisely, we found that the operators $O_{78 \dots 86}$ are redundant and can be expressed in terms of the remaining operators as follows:

$$\begin{aligned}
O_{78} &= \frac{1}{12} (q_1^4 - 4q_1^2 (q_2^2 + q_3^2) + q_2^4 - 4q_2^2 q_3^2 + q_3^4) O_{17} + \frac{\sqrt{3}}{8} (q_1^2 - q_3^2) O_{70} - \frac{1}{8} (q_1^2 - 2q_2^2 + q_3^2) O_{71} \\
&\quad + \frac{1}{2} (q_1^2 + q_2^2 + q_3^2) O_{72} + \frac{1}{4} (q_3^2 - q_1^2) O_{76} + \frac{1}{4\sqrt{3}} (q_1^2 - 2q_2^2 + q_3^2) O_{77} - 2O_{87}, \\
O_{79} &= -\frac{1}{8\sqrt{3}} (q_1^2 - 2q_2^2 + q_3^2) O_{70} + \frac{1}{8} (q_3^2 - q_1^2) O_{71} - \frac{1}{6} (q_1^2 + q_2^2 + q_3^2) O_{73} + \frac{1}{12} (q_1^2 - 2q_2^2 + q_3^2) O_{76} \\
&\quad + \frac{1}{4\sqrt{3}} (q_1^2 - q_3^2) O_{77}, \\
O_{80} &= -\frac{1}{8\sqrt{3}} (q_1^2 - q_3^2) (q_1^2 - 5q_2^2 + q_3^2) O_{17} - \frac{3}{8} q_2^2 O_{70} + \frac{\sqrt{3}}{8} (q_3^2 - q_1^2) O_{71} + \frac{3}{4} q_2^2 O_{74} + \frac{\sqrt{3}}{4} (q_1^2 - q_3^2) O_{75}
\end{aligned}$$

$$\begin{aligned}
& -\frac{\sqrt{3}}{2}q_2^2O_{76} + \frac{1}{2}(q_3^2 - q_1^2)O_{77} - \frac{1}{2}O_{88}, \\
O_{81} &= \frac{1}{24}(q_1^4 + 5q_1^2(q_2^2 - 2q_3^2) - 2q_2^4 + 5q_2^2q_3^2 + q_3^4)O_{17} + \frac{\sqrt{3}}{8}(q_3^2 - q_1^2)O_{70} + \frac{1}{8}(-2q_1^2 + q_2^2 - 2q_3^2)O_{71} \\
&+ \frac{\sqrt{3}}{4}(q_1^2 - q_3^2)O_{74} + \frac{1}{4}(2q_1^2 - q_2^2 + 2q_3^2)O_{75} + \frac{1}{2}(q_3^2 - q_1^2)O_{76} + \frac{1}{2\sqrt{3}}(-2q_1^2 + q_2^2 - 2q_3^2)O_{77} - \frac{1}{2}O_{89}, \\
O_{82} &= \frac{1}{8}(q_1^2 - q_3^2)(q_1^2 - q_2^2 + q_3^2)O_{17} + \frac{1}{8\sqrt{3}}(-2q_1^2 + q_2^2 - 2q_3^2)O_{70} + \frac{1}{8}(q_1^2 - q_3^2)O_{71} + (q_3^2 - q_1^2)O_{72} \\
&- \frac{1}{3}(q_1^2 - 2q_2^2 + q_3^2)O_{73} - \frac{\sqrt{3}}{4}q_2^2O_{74} + \frac{1}{4}(q_3^2 - q_1^2)O_{75} + \frac{1}{6}(q_1^2 + 4q_2^2 + q_3^2)O_{76} + \frac{1}{2\sqrt{3}}(q_1^2 - q_3^2)O_{77} + \frac{\sqrt{3}}{2}O_{88}, \\
O_{83} &= -\frac{1}{8\sqrt{3}}(q_1^4 + q_1^2(q_2^2 - 2q_3^2) - 2q_2^4 + q_2^2q_3^2 + q_3^4)O_{17} + \frac{1}{8}(q_1^2 - q_3^2)O_{70} - \frac{\sqrt{3}}{8}q_2^2O_{71} \\
&+ \frac{1}{\sqrt{3}}(q_1^2 - 2q_2^2 + q_3^2)O_{72} + \frac{1}{\sqrt{3}}(q_3^2 - q_1^2)O_{73} + \frac{1}{4}(q_3^2 - q_1^2)O_{74} + \frac{1}{4\sqrt{3}}(-2q_1^2 + q_2^2 - 2q_3^2)O_{75} \\
&+ \frac{1}{2\sqrt{3}}(q_1^2 - q_3^2)O_{76} + \frac{1}{2}(q_1^2 + q_3^2)O_{77} + \frac{\sqrt{3}}{2}O_{89}, \\
O_{84} &= \frac{1}{12}(q_1^4 - 6q_1^2(q_2^2 + q_3^2) + q_2^4 - 6q_2^2q_3^2 + q_3^4)O_{17} + \frac{\sqrt{3}}{4}(q_1^2 - q_3^2)O_{70} - \frac{1}{4}(q_1^2 - 2q_2^2 + q_3^2)O_{71} \\
&+ (q_1^2 + q_2^2 + q_3^2)O_{72} + \frac{1}{2}(q_3^2 - q_1^2)O_{76} + \frac{1}{2\sqrt{3}}(q_1^2 - 2q_2^2 + q_3^2)O_{77} - 2O_{87}, \\
O_{85} &= \frac{1}{4\sqrt{3}}(q_1^2 - q_3^2)(q_1^2 - 3q_2^2 + q_3^2)O_{17} + \frac{1}{4}(q_1^2 + q_2^2 + q_3^2)O_{70} + \frac{1}{2}(q_1^2 - 2q_2^2 + q_3^2)O_{74} + \frac{\sqrt{3}}{2}(q_3^2 - q_1^2)O_{75} \\
&+ \frac{\sqrt{3}}{2}q_2^2O_{76} + \frac{1}{2}(q_1^2 - q_3^2)O_{77} + O_{88}, \\
O_{86} &= \frac{1}{12}(-q_1^4 - 3q_1^2(q_2^2 - 2q_3^2) + 2q_2^4 - 3q_2^2q_3^2 - q_3^4)O_{17} + \frac{1}{4}(q_1^2 + q_2^2 + q_3^2)O_{71} + \frac{1}{2}\sqrt{3}(q_3^2 - q_1^2)O_{74} \\
&- \frac{1}{2}(q_1^2 - 2q_2^2 + q_3^2)O_{75} + \frac{1}{2}(q_1^2 - q_3^2)O_{76} + \frac{1}{2\sqrt{3}}(2q_1^2 - q_2^2 + 2q_3^2)O_{77} + O_{89}. \tag{2.4}
\end{aligned}$$

One immediately observes from Table I that the operators \mathcal{G}_{20} and \mathcal{G}_{21} are redundant.

Here and in what follows, we adopt the new basis with 80 operators which can be generated by 20 operators given in momentum and coordinate spaces in Table II. For the sake of completeness, we also provide relations between the old and new structure functions \mathcal{F}_i : In order to distinguish the new basis from old one, we from now on label a set of the previous 22 operators and structure functions by “old”. We use the relation

$$\sum_{i=1}^{22} \mathcal{G}_i^{\text{old}} \mathcal{F}_i^{\text{old}}(q_1, q_2, q_3) + 5 \text{ permutations} = \sum_{i=1}^{20} \mathcal{G}_i \mathcal{F}_i(q_1, q_2, q_3) + 5 \text{ permutations} \tag{2.5}$$

to express \mathcal{F}_i in terms of $\mathcal{F}_i^{\text{old}}$ via

$$\begin{aligned}
\mathcal{F}_i(q_1, q_2, q_3) &= \mathcal{F}_i^{\text{old}}(q_1, q_2, q_3) \quad \text{for } i = 1, \dots, 5, 7 \dots 17, \\
\mathcal{F}_6(q_1, q_2, q_3) &= \mathcal{F}_6^{\text{old}}(q_1, q_2, q_3) + \left(\frac{1}{24}q_1^2(q_1^2 - q_2^2 - 3q_3^2)\mathcal{F}_{20}^{\text{old}}(q_1, q_2, q_3) \right. \\
&\quad \left. + \frac{1}{24}q_2^2(-3q_1^2 + q_2^2 - 3q_3^2)\mathcal{F}_{21}^{\text{old}}(q_1, q_2, q_3) + 5 \text{ permutations} \right), \\
\mathcal{F}_{18}(q_1, q_2, q_3) &= \mathcal{F}_{18}^{\text{old}}(q_1, q_2, q_3) + \frac{1}{8}(-q_1^2 + q_2^2 - q_3^2)\mathcal{F}_{20}^{\text{old}}(q_1, q_2, q_3) + \frac{1}{8}(q_1^2 + q_2^2 - q_3^2)\mathcal{F}_{20}^{\text{old}}(q_1, q_3, q_2) \\
&+ \frac{1}{8}(-q_1^2 + q_2^2 + q_3^2)\mathcal{F}_{20}^{\text{old}}(q_3, q_1, q_2) + \frac{1}{8}(-q_1^2 + q_2^2 - q_3^2)\mathcal{F}_{20}^{\text{old}}(q_3, q_2, q_1) \\
&+ \frac{1}{8}(-q_1^2 + q_2^2 - q_3^2)\mathcal{F}_{21}^{\text{old}}(q_1, q_3, q_2) + \frac{1}{8}(-q_1^2 + q_2^2 - q_3^2)\mathcal{F}_{21}^{\text{old}}(q_2, q_1, q_3)
\end{aligned}$$

Generators \mathcal{G} in momentum space	Generators $\tilde{\mathcal{G}}$ in coordinate space
$\mathcal{G}_1 = 1$	$\tilde{\mathcal{G}}_1 = 1$
$\mathcal{G}_2 = \boldsymbol{\tau}_1 \cdot \boldsymbol{\tau}_3$	$\tilde{\mathcal{G}}_2 = \boldsymbol{\tau}_1 \cdot \boldsymbol{\tau}_3$
$\mathcal{G}_3 = \vec{\sigma}_1 \cdot \vec{\sigma}_3$	$\tilde{\mathcal{G}}_3 = \vec{\sigma}_1 \cdot \vec{\sigma}_3$
$\mathcal{G}_4 = \boldsymbol{\tau}_1 \cdot \boldsymbol{\tau}_3 \vec{\sigma}_1 \cdot \vec{\sigma}_3$	$\tilde{\mathcal{G}}_4 = \boldsymbol{\tau}_1 \cdot \boldsymbol{\tau}_3 \vec{\sigma}_1 \cdot \vec{\sigma}_3$
$\mathcal{G}_5 = \boldsymbol{\tau}_2 \cdot \boldsymbol{\tau}_3 \vec{\sigma}_1 \cdot \vec{\sigma}_2$	$\tilde{\mathcal{G}}_5 = \boldsymbol{\tau}_2 \cdot \boldsymbol{\tau}_3 \vec{\sigma}_1 \cdot \vec{\sigma}_2$
$\mathcal{G}_6 = \boldsymbol{\tau}_1 \cdot (\boldsymbol{\tau}_2 \times \boldsymbol{\tau}_3) \vec{\sigma}_1 \cdot (\vec{\sigma}_2 \times \vec{\sigma}_3)$	$\tilde{\mathcal{G}}_6 = \boldsymbol{\tau}_1 \cdot (\boldsymbol{\tau}_2 \times \boldsymbol{\tau}_3) \vec{\sigma}_1 \cdot (\vec{\sigma}_2 \times \vec{\sigma}_3)$
$\mathcal{G}_7 = \boldsymbol{\tau}_1 \cdot (\boldsymbol{\tau}_2 \times \boldsymbol{\tau}_3) \vec{\sigma}_2 \cdot (\vec{q}_1 \times \vec{q}_3)$	$\tilde{\mathcal{G}}_7 = \boldsymbol{\tau}_1 \cdot (\boldsymbol{\tau}_2 \times \boldsymbol{\tau}_3) \vec{\sigma}_2 \cdot (\hat{r}_{12} \times \hat{r}_{23})$
$\mathcal{G}_8 = \vec{q}_1 \cdot \vec{\sigma}_1 \vec{q}_1 \cdot \vec{\sigma}_3$	$\tilde{\mathcal{G}}_8 = \hat{r}_{23} \cdot \vec{\sigma}_1 \hat{r}_{23} \cdot \vec{\sigma}_3$
$\mathcal{G}_9 = \vec{q}_1 \cdot \vec{\sigma}_3 \vec{q}_3 \cdot \vec{\sigma}_1$	$\tilde{\mathcal{G}}_9 = \hat{r}_{23} \cdot \vec{\sigma}_3 \hat{r}_{12} \cdot \vec{\sigma}_1$
$\mathcal{G}_{10} = \vec{q}_1 \cdot \vec{\sigma}_1 \vec{q}_3 \cdot \vec{\sigma}_3$	$\tilde{\mathcal{G}}_{10} = \hat{r}_{23} \cdot \vec{\sigma}_1 \hat{r}_{12} \cdot \vec{\sigma}_3$
$\mathcal{G}_{11} = \boldsymbol{\tau}_2 \cdot \boldsymbol{\tau}_3 \vec{q}_1 \cdot \vec{\sigma}_1 \vec{q}_1 \cdot \vec{\sigma}_2$	$\tilde{\mathcal{G}}_{11} = \boldsymbol{\tau}_2 \cdot \boldsymbol{\tau}_3 \hat{r}_{23} \cdot \vec{\sigma}_1 \hat{r}_{23} \cdot \vec{\sigma}_2$
$\mathcal{G}_{12} = \boldsymbol{\tau}_2 \cdot \boldsymbol{\tau}_3 \vec{q}_1 \cdot \vec{\sigma}_1 \vec{q}_3 \cdot \vec{\sigma}_2$	$\tilde{\mathcal{G}}_{12} = \boldsymbol{\tau}_2 \cdot \boldsymbol{\tau}_3 \hat{r}_{23} \cdot \vec{\sigma}_1 \hat{r}_{12} \cdot \vec{\sigma}_2$
$\mathcal{G}_{13} = \boldsymbol{\tau}_2 \cdot \boldsymbol{\tau}_3 \vec{q}_3 \cdot \vec{\sigma}_1 \vec{q}_1 \cdot \vec{\sigma}_2$	$\tilde{\mathcal{G}}_{13} = \boldsymbol{\tau}_2 \cdot \boldsymbol{\tau}_3 \hat{r}_{12} \cdot \vec{\sigma}_1 \hat{r}_{23} \cdot \vec{\sigma}_2$
$\mathcal{G}_{14} = \boldsymbol{\tau}_2 \cdot \boldsymbol{\tau}_3 \vec{q}_3 \cdot \vec{\sigma}_1 \vec{q}_3 \cdot \vec{\sigma}_2$	$\tilde{\mathcal{G}}_{14} = \boldsymbol{\tau}_2 \cdot \boldsymbol{\tau}_3 \hat{r}_{12} \cdot \vec{\sigma}_1 \hat{r}_{12} \cdot \vec{\sigma}_2$
$\mathcal{G}_{15} = \boldsymbol{\tau}_1 \cdot \boldsymbol{\tau}_3 \vec{q}_2 \cdot \vec{\sigma}_1 \vec{q}_2 \cdot \vec{\sigma}_3$	$\tilde{\mathcal{G}}_{15} = \boldsymbol{\tau}_1 \cdot \boldsymbol{\tau}_3 \hat{r}_{13} \cdot \vec{\sigma}_1 \hat{r}_{13} \cdot \vec{\sigma}_3$
$\mathcal{G}_{16} = \boldsymbol{\tau}_2 \cdot \boldsymbol{\tau}_3 \vec{q}_3 \cdot \vec{\sigma}_2 \vec{q}_3 \cdot \vec{\sigma}_3$	$\tilde{\mathcal{G}}_{16} = \boldsymbol{\tau}_2 \cdot \boldsymbol{\tau}_3 \hat{r}_{12} \cdot \vec{\sigma}_2 \hat{r}_{12} \cdot \vec{\sigma}_3$
$\mathcal{G}_{17} = \boldsymbol{\tau}_1 \cdot \boldsymbol{\tau}_3 \vec{q}_1 \cdot \vec{\sigma}_1 \vec{q}_3 \cdot \vec{\sigma}_3$	$\tilde{\mathcal{G}}_{17} = \boldsymbol{\tau}_1 \cdot \boldsymbol{\tau}_3 \hat{r}_{23} \cdot \vec{\sigma}_1 \hat{r}_{12} \cdot \vec{\sigma}_3$
$\mathcal{G}_{18} = \boldsymbol{\tau}_1 \cdot (\boldsymbol{\tau}_2 \times \boldsymbol{\tau}_3) \vec{\sigma}_1 \cdot \vec{\sigma}_3 \vec{\sigma}_2 \cdot (\vec{q}_1 \times \vec{q}_3)$	$\tilde{\mathcal{G}}_{18} = \boldsymbol{\tau}_1 \cdot (\boldsymbol{\tau}_2 \times \boldsymbol{\tau}_3) \vec{\sigma}_1 \cdot \vec{\sigma}_3 \vec{\sigma}_2 \cdot (\hat{r}_{12} \times \hat{r}_{23})$
$\mathcal{G}_{19} = \boldsymbol{\tau}_1 \cdot (\boldsymbol{\tau}_2 \times \boldsymbol{\tau}_3) \vec{\sigma}_3 \cdot \vec{q}_1 \vec{q}_1 \cdot (\vec{\sigma}_1 \times \vec{\sigma}_2)$	$\tilde{\mathcal{G}}_{19} = \boldsymbol{\tau}_1 \cdot (\boldsymbol{\tau}_2 \times \boldsymbol{\tau}_3) \vec{\sigma}_3 \cdot \hat{r}_{23} \hat{r}_{23} \cdot (\vec{\sigma}_1 \times \vec{\sigma}_2)$
$\mathcal{G}_{20} = \boldsymbol{\tau}_1 \cdot (\boldsymbol{\tau}_2 \times \boldsymbol{\tau}_3) \vec{\sigma}_1 \cdot \vec{q}_1 \vec{\sigma}_3 \cdot \vec{q}_3 \vec{\sigma}_2 \cdot (\vec{q}_1 \times \vec{q}_3)$	$\tilde{\mathcal{G}}_{20} = \boldsymbol{\tau}_1 \cdot (\boldsymbol{\tau}_2 \times \boldsymbol{\tau}_3) \vec{\sigma}_1 \cdot \hat{r}_{23} \vec{\sigma}_3 \cdot \hat{r}_{12} \vec{\sigma}_2 \cdot (\hat{r}_{12} \times \hat{r}_{23})$

TABLE II: The set of 20 generating operators \mathcal{G}_i which generate 80 independent operators O_i of a local three-nucleon force.

$$\begin{aligned}
& + \frac{1}{8} (-q_1^2 + q_2^2 - q_3^2) \mathcal{F}_{21}^{\text{old}}(q_2, q_3, q_1) + \frac{1}{8} (-q_1^2 + q_2^2 - q_3^2) \mathcal{F}_{21}^{\text{old}}(q_3, q_1, q_2) \\
& + \frac{1}{4} q_2^2 \mathcal{F}_{21}^{\text{old}}(q_1, q_2, q_3) + \frac{1}{4} q_2^2 \mathcal{F}_{21}^{\text{old}}(q_3, q_2, q_1), \\
\mathcal{F}_{19}(q_1, q_2, q_3) &= \mathcal{F}_{19}^{\text{old}}(q_1, q_2, q_3) + \frac{1}{4} (-q_1^2 + q_2^2 + 3q_3^2) \mathcal{F}_{20}^{\text{old}}(q_1, q_2, q_3) + \frac{1}{4} (-q_1^2 + 3q_2^2 + q_3^2) \mathcal{F}_{20}^{\text{old}}(q_1, q_3, q_2) \\
& + \frac{1}{4} (q_1^2 - q_2^2 - q_3^2) \mathcal{F}_{20}^{\text{old}}(q_3, q_1, q_2) + \frac{1}{4} (q_1^2 - q_2^2 + q_3^2) \mathcal{F}_{20}^{\text{old}}(q_3, q_2, q_1) \\
& + \frac{1}{4} (q_1^2 - q_2^2 + q_3^2) \mathcal{F}_{21}^{\text{old}}(q_1, q_3, q_2) + \frac{1}{4} (-q_1^2 + q_2^2 + 3q_3^2) \mathcal{F}_{21}^{\text{old}}(q_2, q_1, q_3) \\
& + \frac{1}{4} (q_1^2 - q_2^2 + q_3^2) \mathcal{F}_{21}^{\text{old}}(q_2, q_3, q_1) + \frac{1}{4} (-q_1^2 + q_2^2 + 3q_3^2) \mathcal{F}_{21}^{\text{old}}(q_3, q_1, q_2) \\
& + \frac{1}{2} q_2^2 \mathcal{F}_{21}^{\text{old}}(q_1, q_2, q_3) + \frac{1}{2} q_2^2 \mathcal{F}_{21}^{\text{old}}(q_3, q_2, q_1), \\
\mathcal{F}_{20}(q_1, q_2, q_3) &= \mathcal{F}_{22}^{\text{old}}(q_1, q_2, q_3) - \frac{1}{2} \mathcal{F}_{20}^{\text{old}}(q_1, q_2, q_3) - \frac{1}{2} \mathcal{F}_{20}^{\text{old}}(q_1, q_3, q_2) - \frac{1}{2} \mathcal{F}_{20}^{\text{old}}(q_3, q_1, q_2) - \frac{1}{2} \mathcal{F}_{20}^{\text{old}}(q_3, q_2, q_1) \\
& - \frac{1}{2} \mathcal{F}_{21}^{\text{old}}(q_1, q_3, q_2) - \frac{1}{2} \mathcal{F}_{21}^{\text{old}}(q_2, q_1, q_3) - \frac{1}{2} \mathcal{F}_{21}^{\text{old}}(q_2, q_3, q_1) - \frac{1}{2} \mathcal{F}_{21}^{\text{old}}(q_3, q_1, q_2). \tag{2.6}
\end{aligned}$$

Analogously, in coordinate space we have

$$\sum_{i=1}^{22} \tilde{\mathcal{G}}_i^{\text{old}} \mathcal{F}_i^{\text{old}}(r_{12}, r_{23}, r_{31}) + 5 \text{ permutations} = \sum_{i=1}^{20} \tilde{\mathcal{G}}_i \mathcal{F}_i(r_{12}, r_{23}, r_{31}) + 5 \text{ permutations}, \tag{2.7}$$

so that \mathcal{F}_i can be expressed in terms of $\mathcal{F}_i^{\text{old}}$ via

$$\begin{aligned}
\mathcal{F}_i(r_{12}, r_{23}, r_{31}) &= \mathcal{F}_i^{\text{old}}(r_{12}, r_{23}, r_{31}) \quad \text{for } i = 1 \dots 5, 7 \dots 17, \\
\mathcal{F}_6(r_{12}, r_{23}, r_{31}) &= \mathcal{F}_6^{\text{old}}(r_{12}, r_{23}, r_{31}) + \left(\frac{1}{24} r_{23}^2 (3r_{12}^2 + r_{31}^2 - r_{23}^2) \mathcal{F}_{20}^{\text{old}}(r_{12}, r_{23}, r_{31}) \right.
\end{aligned}$$

$$\begin{aligned}
& + \frac{1}{24} r_{31}^2 (3r_{12}^2 - r_{31}^2 + 3r_{23}^2) \mathcal{F}_{21}^{\text{old}}(r_{12}, r_{23}, r_{31}) + 5 \text{ permutations} \Big), \\
\mathcal{F}_{18}(r_{12}, r_{23}, r_{31}) &= \mathcal{F}_{18}^{\text{old}}(r_{12}, r_{23}, r_{31}) + \frac{1}{8} (-r_{12}^2 - r_{23}^2 + r_{31}^2) \mathcal{F}_{20}^{\text{old}}(r_{12}, r_{23}, r_{31}) \\
& + \frac{1}{8} (-r_{12}^2 - r_{23}^2 + r_{31}^2) \mathcal{F}_{20}^{\text{old}}(r_{23}, r_{12}, r_{31}) + \frac{1}{8} (r_{12}^2 - r_{23}^2 + r_{31}^2) \mathcal{F}_{20}^{\text{old}}(r_{31}, r_{12}, r_{23}) \\
& + \frac{1}{8} (-r_{12}^2 + r_{23}^2 + r_{31}^2) \mathcal{F}_{20}^{\text{old}}(r_{31}, r_{23}, r_{12}) + \frac{1}{8} (-r_{12}^2 - r_{23}^2 + r_{31}^2) \mathcal{F}_{21}^{\text{old}}(r_{12}, r_{31}, r_{23}) \\
& + \frac{1}{8} (-r_{12}^2 - r_{23}^2 + r_{31}^2) \mathcal{F}_{21}^{\text{old}}(r_{23}, r_{31}, r_{12}) + \frac{1}{8} (-r_{12}^2 - r_{23}^2 + r_{31}^2) \mathcal{F}_{21}^{\text{old}}(r_{31}, r_{12}, r_{23}) \\
& + \frac{1}{8} (-r_{12}^2 - r_{23}^2 + r_{31}^2) \mathcal{F}_{21}^{\text{old}}(r_{31}, r_{23}, r_{12}) + \frac{1}{4} r_{31}^2 \mathcal{F}_{21}^{\text{old}}(r_{12}, r_{23}, r_{31}) + \frac{1}{4} r_{31}^2 \mathcal{F}_{21}^{\text{old}}(r_{23}, r_{12}, r_{31}), \\
\mathcal{F}_{19}(r_{12}, r_{23}, r_{31}) &= \mathcal{F}_{19}^{\text{old}}(r_{12}, r_{23}, r_{31}) + \frac{1}{4} (-3r_{12}^2 + r_{23}^2 - r_{31}^2) \mathcal{F}_{20}^{\text{old}}(r_{12}, r_{23}, r_{31}) \\
& + \frac{1}{4} (-r_{12}^2 - r_{23}^2 + r_{31}^2) \mathcal{F}_{20}^{\text{old}}(r_{23}, r_{12}, r_{31}) + \frac{1}{4} (r_{12}^2 - r_{23}^2 + r_{31}^2) \mathcal{F}_{20}^{\text{old}}(r_{31}, r_{12}, r_{23}) \\
& + \frac{1}{4} (-r_{12}^2 + r_{23}^2 - 3r_{31}^2) \mathcal{F}_{20}^{\text{old}}(r_{31}, r_{23}, r_{12}) + \frac{1}{4} (-3r_{12}^2 + r_{23}^2 - r_{31}^2) \mathcal{F}_{21}^{\text{old}}(r_{12}, r_{31}, r_{23}) \\
& + \frac{1}{4} (-r_{12}^2 - r_{23}^2 + r_{31}^2) \mathcal{F}_{21}^{\text{old}}(r_{23}, r_{31}, r_{12}) + \frac{1}{4} (-3r_{12}^2 + r_{23}^2 - r_{31}^2) \mathcal{F}_{21}^{\text{old}}(r_{31}, r_{12}, r_{23}) \\
& + \frac{1}{4} (-r_{12}^2 - r_{23}^2 + r_{31}^2) \mathcal{F}_{21}^{\text{old}}(r_{31}, r_{23}, r_{12}) - \frac{1}{2} r_{31}^2 \mathcal{F}_{21}^{\text{old}}(r_{12}, r_{23}, r_{31}) - \frac{1}{2} r_{31}^2 \mathcal{F}_{21}^{\text{old}}(r_{23}, r_{12}, r_{31}), \\
\mathcal{F}_{20}(r_{12}, r_{23}, r_{31}) &= \mathcal{F}_{22}^{\text{old}}(r_{12}, r_{23}, r_{31}) - \frac{1}{2} \mathcal{F}_{20}^{\text{old}}(r_{12}, r_{23}, r_{31}) - \frac{1}{2} \mathcal{F}_{20}^{\text{old}}(r_{23}, r_{12}, r_{31}) - \frac{1}{2} \mathcal{F}_{20}^{\text{old}}(r_{31}, r_{12}, r_{23}) \\
& - \frac{1}{2} \mathcal{F}_{20}^{\text{old}}(r_{31}, r_{23}, r_{12}) - \frac{1}{2} \mathcal{F}_{21}^{\text{old}}(r_{12}, r_{31}, r_{23}) - \frac{1}{2} \mathcal{F}_{21}^{\text{old}}(r_{23}, r_{31}, r_{12}) - \frac{1}{2} \mathcal{F}_{21}^{\text{old}}(r_{31}, r_{12}, r_{23}) \\
& - \frac{1}{2} \mathcal{F}_{21}^{\text{old}}(r_{31}, r_{23}, r_{12}). \tag{2.8}
\end{aligned}$$

III. CHIRAL EXPANSION OF THE THREE-NUCLEON FORCE IN COORDINATE SPACE

We are now in the position to discuss the contributions of the long- and intermediate-range 3NF topologies to the structure functions $\mathcal{F}_i(r_{31}, r_{23}, r_{12})$.

We begin with the longest-range 2π -exchange 3NF whose explicit expressions at $N^2\text{LO}$, $N^3\text{LO}$ and $N^4\text{LO}$ are given in Ref. [22] both in momentum and coordinate spaces. Following the lines of Ref. [2], we restrict ourselves in this qualitative discussion to the equilateral triangle configuration with $r_{12} = r_{23} = r_{31} \equiv r$ which allows us to visualize the structure functions in a simple way. Notice that while this is sufficient for a qualitative estimation of the size of various contributions, the final conclusions about the importance of the individual structures in the 3NF for nuclear observables can only be drawn upon solving the quantum-mechanical A -body problem. Work along these lines is in progress, see [20, 21] for some preliminary results.

In Fig. 1 we show the chiral expansion of the structure functions $\mathcal{F}_i(r)$ generated by the 2π -exchange 3NF topology up to $N^4\text{LO}$. Here and in what follows, we use the values for the various LECs from Ref. [22] corresponding to the order- Q^4 fit to pion-nucleon phase shifts from the Karsruhe-Helsinki (KH) partial-wave analysis [23]. Specifically, we use $M_\pi = 138$ MeV, $F_\pi = 92.4$ MeV, $g_A = 1.285^2$ for the pion mass, pion decay constant and the nucleon axial vector coupling while the values of the other relevant LECs are: $c_1 = -0.75$ GeV^{-1} , $c_2 = 3.49$ GeV^{-1} , $c_3 = -4.77$ GeV^{-1} , $c_4 = 3.34$ GeV^{-1} , $\bar{e}_{14} = -1.52$ GeV^{-3} and $\bar{e}_{17} = -0.37$ GeV^{-3} . Notice that while the function $\mathcal{F}_i(r)$ are shown in the range of $1 \dots 3$ fm, the chiral expansion for the potentials is expected to converge only at sufficiently large distances, see Ref. [24] for a related discussion. The most recent versions of the chiral nucleon-nucleon potentials employ local

² This value takes into account the Goldberger-Treiman discrepancy.

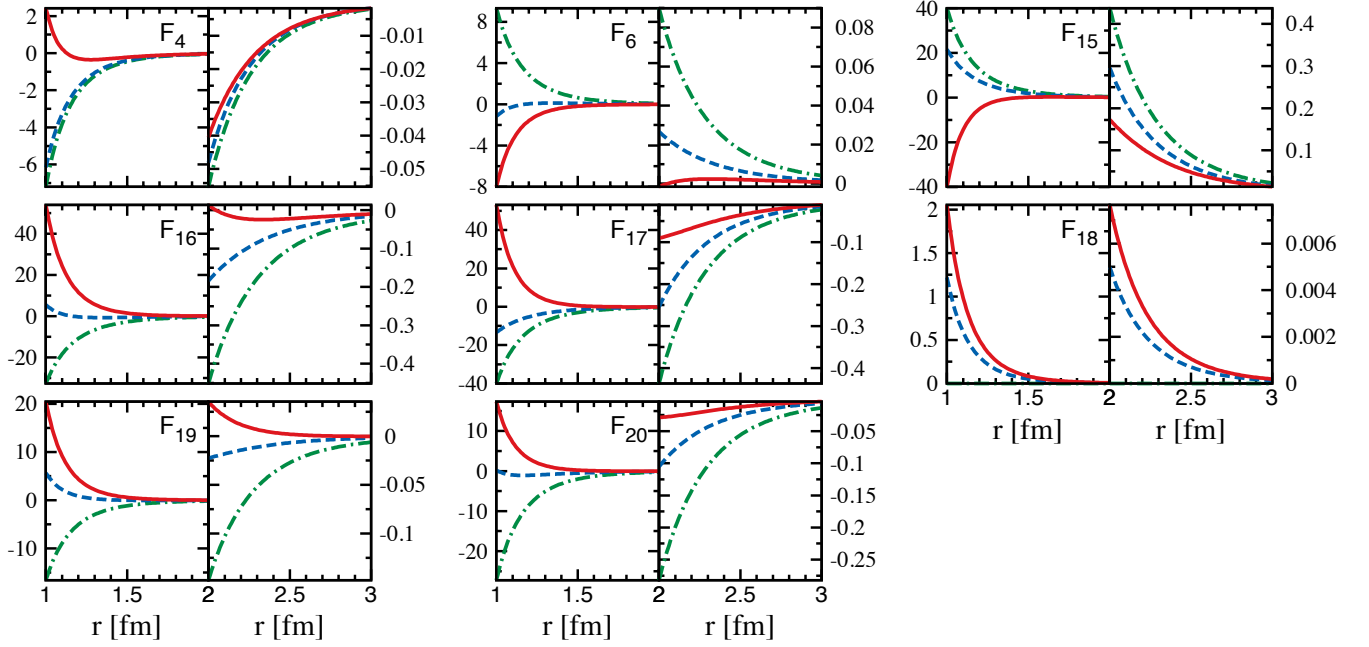


FIG. 1: Chiral expansion of the profile functions $\mathcal{F}_i(r)$ in MeV generated by the two-pion exchange 3NF topology up to N^4 LO (in the equilateral triangle configuration). Dashed-dotted, dashed and solid lines correspond to $\mathcal{F}_i^{(3)}$, $\mathcal{F}_i^{(3)} + \mathcal{F}_i^{(4)}$ and $\mathcal{F}_i^{(3)} + \mathcal{F}_i^{(4)} + \mathcal{F}_i^{(5)}$, respectively.

regularization of the pion-exchange contributions in coordinate space with the cutoff $R_0 \sim 1$ fm [25, 26]. Such a regulator would clearly strongly affect the behavior of the functions $\mathcal{F}_i(r)$ at short distances but would have little impact at relative distances $r > 2$ fm.

The 2π -exchange topology gives rise to 8 out of 20 operators. Surprisingly, one observes that the chiral expansion only appears to converge at this order for rather large distances beyond $r \sim 2.5$ fm. At such distances, the N^4 LO corrections are indeed considerably smaller than the N^3 LO ones. In this context, it is important to keep in mind that contrary to the N^3 LO corrections, the N^4 LO ones involve terms proportional to the LECs $c_{2,3,4}$ which receive contributions from the Δ isobar and appear to be numerically large. Thus, one may indeed expect the N^4 LO contributions to be larger than what is suggested by naive dimensional analysis which, at least to some extent, may explain the observed convergence pattern. The convergence of the chiral expansion for the 2π -exchange 3NF was also addressed in Ref. [22] based on the momentum-space expressions for the function $\mathcal{A}(q_2)$ and $\mathcal{B}(q_2)$, which parametrize the pion-nucleon amplitude in the kinematics relevant to the 3NF. One observes from Fig. 5 of that work that the N^4 LO contributions to both of these functions are significantly smaller than the N^3 LO ones in the range of momentum transfers of $q_2 < 300$ MeV. Confronting these findings with results in coordinate space suggests that higher-momentum components do significantly affect the potential at relative distances of the order of $r \sim 2$ fm, see Ref. [27] for a related discussion.

We also observe an interesting feature that the N^3 LO and N^4 LO corrections contribute in the same direction and lead to a strong reduction in magnitude of the strength of the potentials at distances of the order of $r \sim 2$ fm. For example, the strongest potentials $\mathcal{F}_{15}(r)$, $\mathcal{F}_{16}(r)$ and $\mathcal{F}_{17}(r)$ have, at the relative distance $r = 2$ fm, the strength of 440 keV, -450 keV and -440 keV at N^2 LO while 170 keV, 14 keV and -90 keV at N^4 LO. This feature, that the N^2 LO results based on the c_i 's taken from the order- Q^4 fit to pion-nucleon phase shifts tend to strongly overshoot the 2π -exchange 3NF contribution, is consistent with the observations of Ref. [22] in momentum space.

The results for the 2π - 1π exchange and ring topologies are depicted in Figs. 2 and 3, respectively. Given that these are genuine one-loop topologies, the chiral expansion for these contributions starts at N^3 LO. Notice further that only the results for $\mathcal{F}_{6,19,20}$ are affected by using the new operator basis, see Eq. (2.6) for explicit expressions. Thus, all

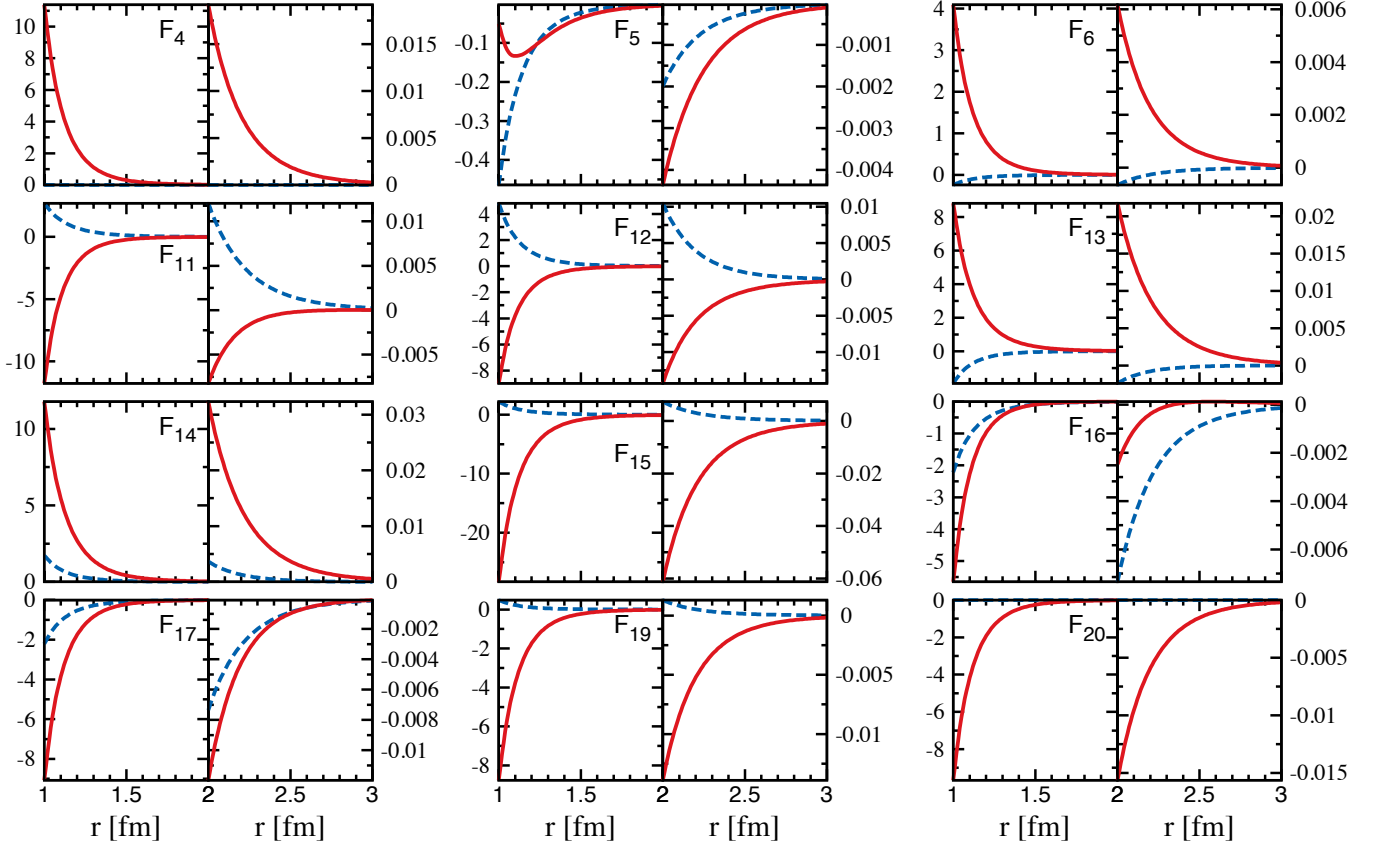


FIG. 2: Chiral expansion of the profile functions $\mathcal{F}_i(r)$ in MeV generated by the two-pion-one-pion exchange 3NF topology up to N^4 LO (in the equilateral triangle configuration). Dashed and solid lines correspond to $\mathcal{F}_i^{(4)}$ and $\mathcal{F}_i^{(4)} + \mathcal{F}_i^{(5)}$, respectively.

conclusions of Ref. [2] remain unaffected. In particular, one observes that the N^4 LO terms are in most cases larger in magnitude than the (nominally) leading contributions at N^3 LO. This pattern is in line with the assumption that these contributions are, to a large extent, driven by intermediate Δ excitations. In the Δ -less formulation of chiral EFT, these effects for the considered 3NF topologies start to appear at N^4 LO.

It is instructive to compare the potentials at large distances emerging from the individual topologies with each other. This is visualized in Fig. 4 where only N^4 LO results for the functions \mathcal{F}_i are shown. One clearly observes the longest-range nature of the 2π -exchange 3NF which, in all cases where it doesn't vanish, dominates the potential at distances larger than $r = 2$ fm. In particular, the strongest 2π -exchange potentials $\mathcal{F}_{15}(2 \text{ fm}) \simeq 170 \text{ keV}$, $\mathcal{F}_{17}(2 \text{ fm}) \simeq -90 \text{ keV}$ are considerably larger in magnitude than the strongest 2π - 1π $\mathcal{F}_{14}(2 \text{ fm}) \simeq 29 \text{ keV}$, $\mathcal{F}_{15}(2 \text{ fm}) \simeq -69 \text{ keV}$ and ring potentials $\mathcal{F}_8(2 \text{ fm}) \simeq -60 \text{ keV}$, $\mathcal{F}_{10}(2 \text{ fm}) \simeq -41 \text{ keV}$, respectively. This dominance becomes more pronounced at larger distances while at shorter ones all three topologies generate contributions of a comparable size. We emphasize once again that more quantitative conclusions about importance of individual 3NF contributions can only be drawn upon performing explicit calculations of few-nucleon observables.

Finally, Fig. 5 shows the resulting chiral expansion of the structure functions \mathcal{F}_i when all three types of contributions are added together. These plots clearly reflect the behavior observed for individual topologies as discussed above. The strongest potentials at $r = 2$ fm are $\mathcal{F}_{15} \simeq 100 \text{ keV}$ and $\mathcal{F}_{17} \simeq -90 \text{ keV}$, while at $r \sim M_\pi^{-1} \sim 1.4 \text{ fm}$ one has $\mathcal{F}_{16} \simeq 2.9 \text{ MeV}$ and $\mathcal{F}_{17} \simeq 1.4 \text{ MeV}$.

As already pointed out in Ref. [2], given the large corrections at the subleading one-loop level, i.e. N^4 LO, which are driven by single-delta excitations, it is important to study contributions emerging from intermediate double- and triple- Δ excitations. In the standard Δ -less formulation of chiral EFT, such contributions first appear at N^5 LO and

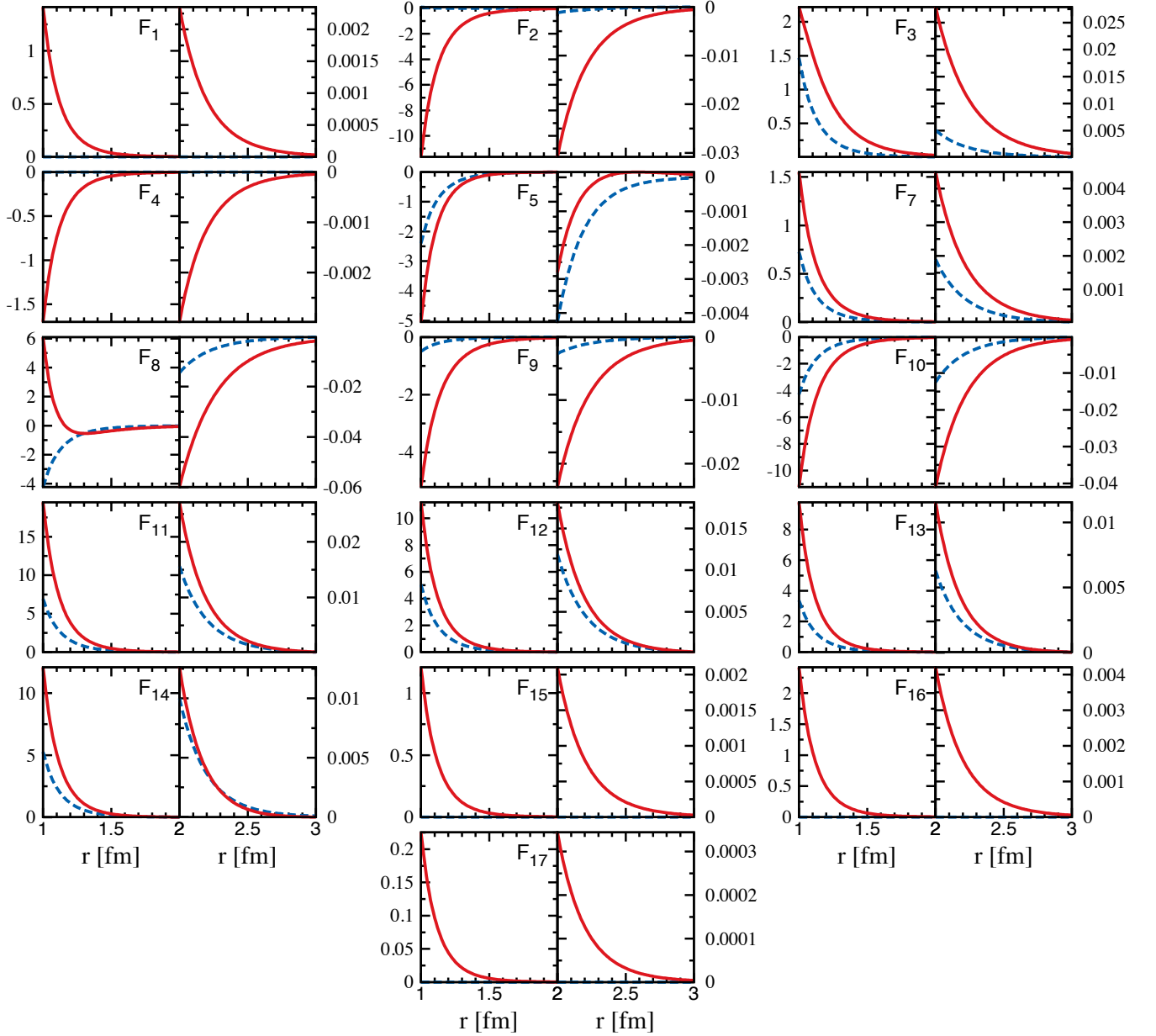


FIG. 3: Chiral expansion of the profile functions $\mathcal{F}_i(r)$ in MeV generated by the ring 3NF topology up to N^4 LO (in the equilateral triangle configuration). Dashed and solid lines correspond to $\mathcal{F}_i^{(4)}$ and $\mathcal{F}_i^{(4)} + \mathcal{F}_i^{(5)}$, respectively.

N^6 LO, respectively, where one would also need to evaluate all possible two-loop diagrams. This is clearly a rather challenging task. A more promising and feasible approach would be to employ the formulation of EFT with explicit Δ degrees of freedom. Such a framework was shown in the past to be quite efficient in resumming the large contributions to the nuclear force associated with intermediate Δ excitations [28–32]. In this formulation, effects of single-, double- and triple- Δ excitations are accounted for at the leading one-loop level, i.e. N^3 LO. Work along these lines is in progress.

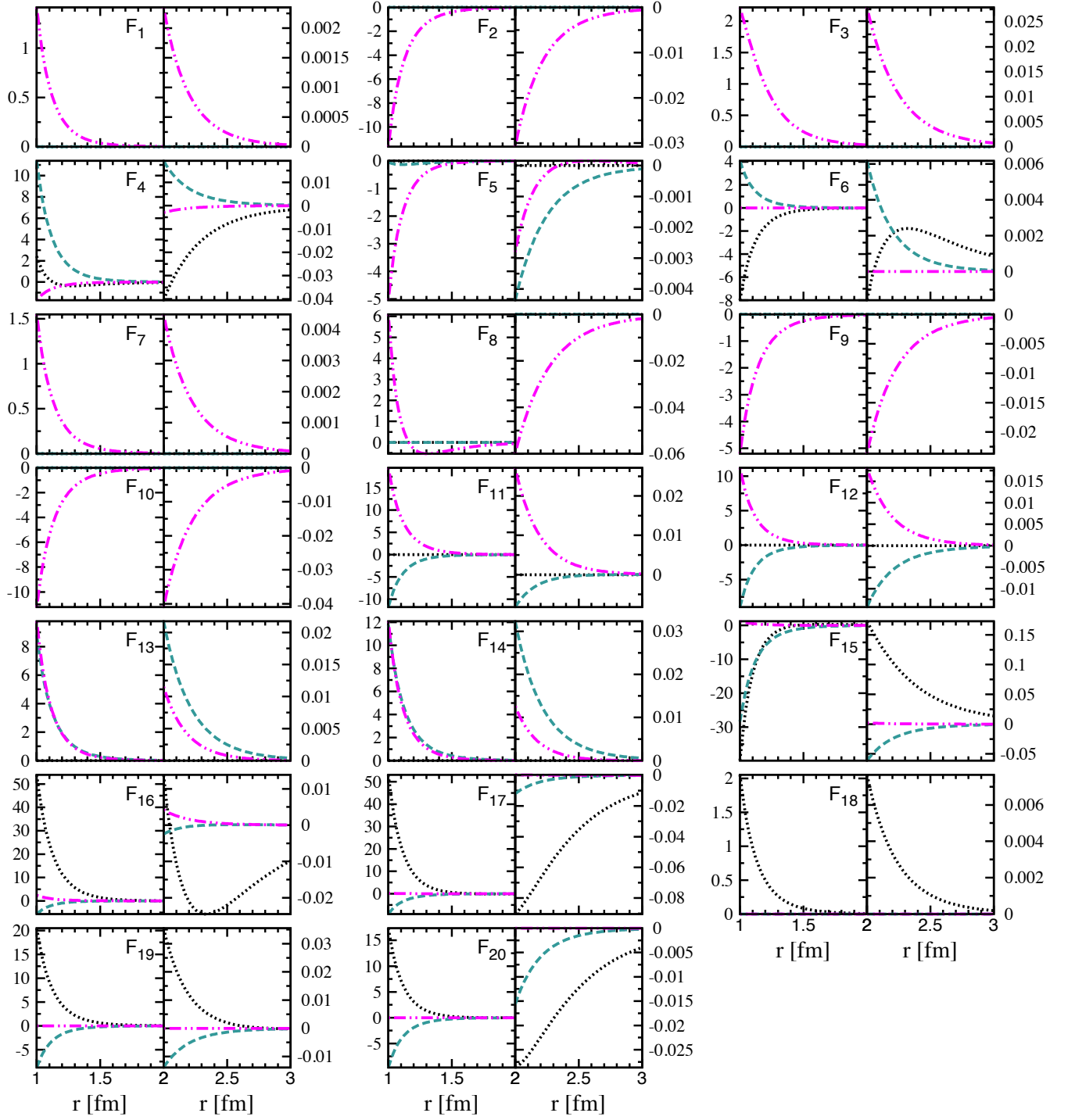


FIG. 4: Individual contributions of the two-pion exchange (dotted lines), two-pion-one-pion exchange (long-dashed lines) and ring (dashed-double-dotted lines) topologies to the profile functions $\mathcal{F}_i(r)$ in MeV at N⁴LO in the equilateral triangle configuration.

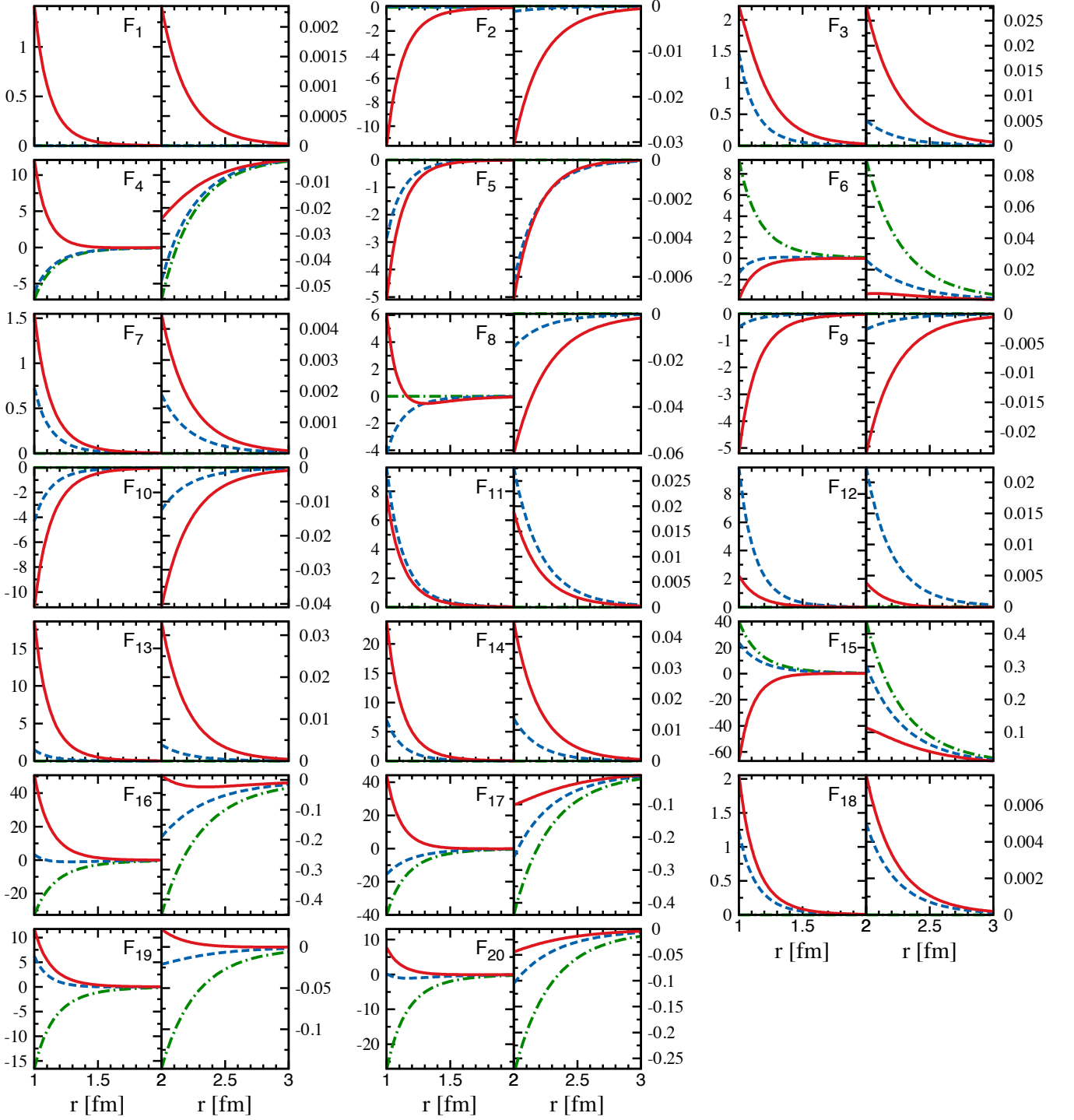


FIG. 5: Chiral expansion of the profile functions $\mathcal{F}_i(r)$ in MeV emerging from all long-range 3NF topologies up to N^4 LO (in the equilateral triangle configuration). Dashed-dotted, dashed and solid lines correspond to $\mathcal{F}_i^{(3)}$, $\mathcal{F}_i^{(3)} + \mathcal{F}_i^{(4)}$ and $\mathcal{F}_i^{(3)} + \mathcal{F}_i^{(4)} + \mathcal{F}_i^{(5)}$, respectively.

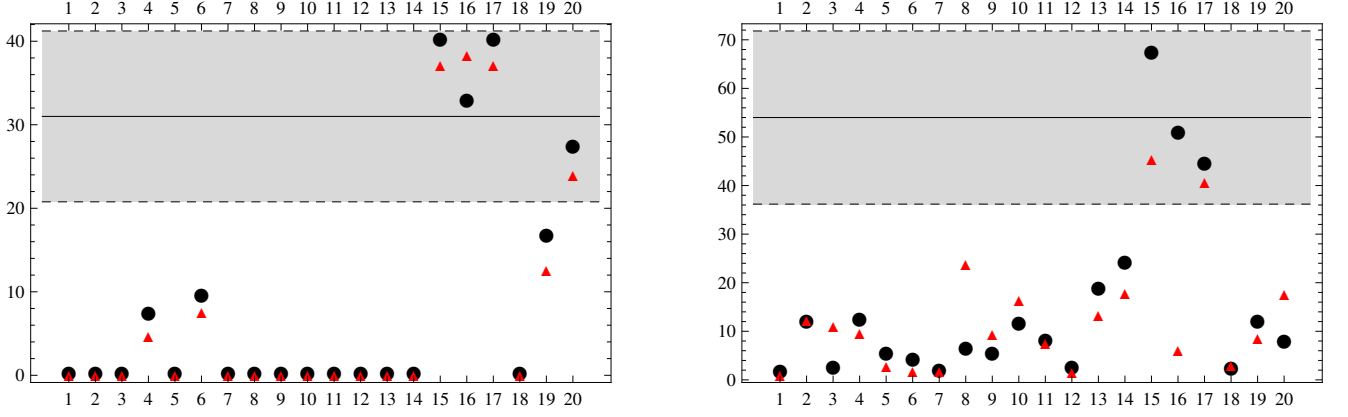


FIG. 6: Absolute values of the profile functions \mathcal{F}_i , with $i = 1, \dots, 20$ shown on the x axis, in the equilateral triangle configuration at the relative distance of $r = 1$ fm (black dots) and $r = 2$ fm (red triangles) at $N^2\text{LO}$ in the left panel and at $N^4\text{LO}$ in the right panel. The values at $r = 1$ fm are shown in units of MeV while the ones at $r = 2$ fm are in units of $1/85$ MeV (left panel) and $1/400$ MeV (right panel). The gray band corresponds to a 30 % uncertainty due to subleading $1/N_c$ -corrections.

IV. LARGE- N_c INSIGHTS

It is interesting to analyze our findings for the profile functions in the light of the $1/N_c$ -expansion of QCD. The final results summarized in Fig. 5 show clearly that not all profile functions are of the same size. In particular, at $r \sim 1$ fm, the absolute values of the functions $|\mathcal{F}_{15,16,17}| \gtrsim 40$ MeV appear to be much larger than the other \mathcal{F}_i 's for no apparent reason. As we will argue below, this pattern is in line with the large- N_c picture of the 3NF.

The large- N_c expansion of QCD proved to be a useful approach for understanding various qualitative aspects of mesons and baryons [33, 34], see Ref. [35] for a review article. In particular, it was applied in Refs. [36, 37] to explain the pattern in the relative strengths of various spin-flavor components of the nucleon-nucleon force as observed in phenomenological models. Recently, these studies were extended to the 3NF [1] by classifying the operators appearing in the 3NF according to their large- N_c scaling. It is thus interesting to confront these insights with the chiral EFT calculations presented in this work. We recall that according to the analysis of Ref. [1], the operators $\mathcal{G}_{1,4,6,15,16,17,18,19,20}$ appear at leading order $\mathcal{O}(N_c)$ while all other structures in Table II appear at subleading order $\mathcal{O}(1/N_c)$. Thus, the observed numerical dominance of $|\mathcal{F}_{15,16,17}|$ is consistent with the corresponding operators contributing at leading order in the large- N_c scaling. While some of the other profile functions for the order- $\mathcal{O}(N_c)$ structures come out smaller, this does not imply a violation of the N_c -scaling.

In order to get further insights into the hierarchy of various profile functions, we plot in Fig. 6 the absolute values of the corresponding potentials in the equilateral triangle configuration at distances of $r = 1$ fm and $r = 2$ fm at $N^2\text{LO}$ (left panel) and $N^4\text{LO}$ (right panel). Here, the horizontal black line is the average of $|\mathcal{F}_{15,16,17,19,20}|$ (left panel) and $|\mathcal{F}_{15,16,17}|$ (right panel) at $r = 1$ fm and serves as an estimation of the natural size of $|\mathcal{F}_i^{(3)}|$ and $|\mathcal{F}_i^{(3)} + \mathcal{F}_i^{(4)} + \mathcal{F}_i^{(5)}|$ at that distance. At $N^2\text{LO}$, the observed hierarchy of the various flavor-spin-space structures in the 3NF is in a good agreement with the expected pattern based on the large- N_c analysis. In particular, except for \mathcal{F}_1 and \mathcal{F}_{18} , all profile functions corresponding to the leading in the $1/N_c$ -counting structures receive sizable contributions at $N^2\text{LO}$. This should not come as a surprise: indeed, it was shown in Ref. [1] that the dominant, i.e. order $\sim N_c$, 3NF contains all operators present in the Fujita-Miyazawa 3NF model [38], which has the same structure as the leading chiral 2π -exchange 3NF, see Eqs. (3.3) and (3.5) of Ref. [22]. In fact, given that $g_A \sim \mathcal{O}(N_c)$ and $F_\pi \sim \mathcal{O}(N_c^{1/2})$, one can immediately read off from these expressions that the $N^2\text{LO}$ 2π -exchange 3NF is of order $\mathcal{O}(N_c)$ in the regime of $|\vec{p}_i| \sim \mathcal{O}(N_c^0)$. Here we assumed that the LECs c_i scale as $c_i \sim \mathcal{O}(N_c)$ which can be verified e.g. within the resonance

saturation picture as discussed in Ref. [39].³ Notice further that the eight coordinate-space profile functions for the 2π -exchange 3NF discussed above emerge from just two flavor-spin-momentum structures $\mathcal{G}_{17,20}$ upon making a Fourier transformation.

At N^4 LO, the profile functions show a qualitatively similar pattern to the one observed at N^2 LO and discussed above, but the picture is not that clear anymore. While the strongest potentials are still the ones corresponding to the operators $\tilde{\mathcal{G}}_{15,16,17}$ which appear at leading order $\mathcal{O}(N_c)$, the remaining weaker potentials show no clear pattern with respect to the large- N_c counting. It should, however, be emphasized that beyond N^2 LO, higher-order diagrams with a larger number of vertices scale with increasingly higher powers of N_c , which naively seems to destroy the $1/N_c$ hierarchy. As it is well known [40, 41], consistency requires delicate cancellations from Δ intermediate states, that at the one loop level and in the one-nucleon sector are currently subject to investigation [42]. Large- N_c consistency was also verified within the boson-exchange picture of the nucleon-nucleon interaction in Refs. [43–45] at the three-meson exchange level provided the potential is defined in a specific way. It remains to be seen whether the large- N_c consistency holds true for nuclear potentials defined with the method of unitary transformation [46, 47]. Irrespective of this issue, we further emphasize that the large- N_c insights into nuclear forces of Refs. [1, 36, 37, 43–45] are achieved assuming the regime in which typical momenta of the nucleons are $|\vec{p}| \sim \mathcal{O}(N_c^0)$, and the Δ -isobar has to be treated as an explicit degree of freedom since $m_\Delta - m_N \sim \mathcal{O}(N_c^{-1})$. These conditions differ substantially from the ones underlying our chiral EFT calculations where, in particular, we assign $|\vec{p}| \sim M_\pi \ll m_\Delta - m_N$. It is conceivable that the impact of this mismatch increases with increasing the chiral order so that the comparison between the two approaches beyond N^2 LO should be taken with care.

V. SUMMARY AND OUTLOOK

The pertinent results of our study can be summarized as follows:

- We have clarified the issue with the different number of operators needed to parametrize the most general isospin-invariant local 3NF reported in Refs. [1, 2]. In particular, we have shown that 2 out of 22 operators listed in Ref. [2] are redundant so that the operator basis involves 20 flavor-spin-space or, equivalently, flavor-spin-momentum operators. This agrees with the findings of Ref. [1]. We also provided explicit expressions which can be used to rewrite the two redundant structures in terms of the remaining 20 operators.
- We re-considered the results for the long- and intermediate-range 3NF up to N^4 LO of Ref. [2] using this new operator basis. In particular, we discussed in detail the convergence of the chiral expansion for the corresponding profile functions in the equilateral triangle topology. As expected, we found large N^4 LO contributions to the 2π - 1π exchange and ring topologies. Moreover, somewhat surprisingly, the N^4 LO corrections to the longest-range 2π exchange topology are found to be still sizable even at relatively large distances. Furthermore, we found that taking into account N^3 LO and N^4 LO corrections to the 2π exchange 3NF amounts to a considerable reduction of the strength of nearly all profile functions at large distances and thus makes the 3NF more short-ranged. Comparing the potentials generated by the individual topologies with each other, we observe a clear dominance of the longest range 2π exchange at distances of $r > 2$ fm, while at short distances of $r \sim 1$ fm the contributions of 2π - 1π and ring graphs start becoming comparable in size. We also see that the 2π - 1π exchange and the ring topologies generate sizable intermediate-range potentials in those structures where the 2π exchange does not contribute.
- We found that the obtained results for the longest- and intermediate-range topologies agree at the qualitative level with the results of the large- N_c analysis of Ref. [1]. We argued that a more quantitative comparison between the two approaches might be difficult due to the different kinematical regimes assumed in the two methods.

The present study represents an important intermediate step towards high-precision analysis of the 3NF in chiral EFT and should be extended in different ways. First, one needs to work out the remaining one-pion-exchange-contact

³ Notice that for the sake of the large- N_c estimations of the LECs $c_{2,3,4}$, it is not legitimate to employ the expansion in powers of $M_\pi/(m_\Delta - m_N)$ as done in Δ -less formulations of chiral effective field theory.

and two-pion-exchange-contact contributions to the 3NF. Together with the results reported in Refs. [2, 22, 48], this will provide a complete representation of the 3NF at N^4 LO. Independently of these studies, one should analyze the 3NF at N^3 LO employing the formulation of chiral EFT where the Δ -isobar is explicitly taken into account [28–31]. A detailed comparison between the two approaches will shed light on the convergence of the chiral expansion and allow one to draw conclusions about the size of higher-order terms and delta-contributions. Finally and most importantly, the resulting novel terms in the 3NF should be partial wave decomposed [49] and employed in *ab-initio* few- and many-body calculations of nuclear reactions and light nuclei, see Refs. [20, 21] for first steps in that direction. Work along these lines is in progress.

Acknowledgments

This work is supported by the EU HadronPhysics3 project “Study of strongly interacting matter”, by the European Research Council (ERC-2010-StG 259218 NuclearEFT) and by the DFG (TR 16, “Subnuclear Structure of Matter”).

-
- [1] D. R. Phillips and C. Schat, Phys. Rev. C **88**, 034002 (2013) [arXiv:1307.6274 [nucl-th]].
 - [2] H. Krebs, A. Gasparyan and E. Epelbaum, Phys. Rev. C **87**, 054007 (2013) [arXiv:1302.2872 [nucl-th]].
 - [3] N. Kalantar-Nayestanaki, E. Epelbaum, J. G. Messchendorp and A. Nogga, Rept. Prog. Phys. **75**, 016301 (2012) [arXiv:1108.1227 [nucl-th]].
 - [4] H.-W. Hammer, A. Nogga and A. Schwenk, Rev. Mod. Phys. **85**, 197 (2013) [arXiv:1210.4273 [nucl-th]].
 - [5] P. Navratil, V. G. Gueorguiev, J. P. Vary, W. E. Ormand and A. Nogga, Phys. Rev. Lett. **99**, 042501 (2007) [nucl-th/0701038].
 - [6] S. C. Pieper, Riv. Nuovo Cim. **31**, 709 (2008) [arXiv:0711.1500 [nucl-th]].
 - [7] K. Hebeler and A. Schwenk, Phys. Rev. C **82**, 014314 (2010) [arXiv:0911.0483 [nucl-th]].
 - [8] E. Epelbaum, H. Krebs, D. Lee and U.-G. Meißner, Eur. Phys. J. A **41**, 125 (2009) [arXiv:0903.1666 [nucl-th]].
 - [9] P. Maris, J. P. Vary, P. Navratil, W. E. Ormand, H. Nam and D. J. Dean, Phys. Rev. Lett. **106**, 202502 (2011) [arXiv:1101.5124 [nucl-th]].
 - [10] R. Roth, J. Langhammer, A. Calci, S. Binder and P. Navratil, Phys. Rev. Lett. **107**, 072501 (2011) [arXiv:1105.3173 [nucl-th]].
 - [11] W. Glöckle, H. Witala, D. Huber, H. Kamada and J. Golak, Phys. Rept. **274**, 107 (1996).
 - [12] S. R. Beane, E. Chang, S. D. Cohen, W. Detmold, H. W. Lin, T. C. Luu, K. Orginos and A. Parreno *et al.*, Phys. Rev. D **87**, no. 3, 034506 (2013) [arXiv:1206.5219 [hep-lat]].
 - [13] E. Epelbaum, H. -W. Hammer and U.-G. Meißner, Rev. Mod. Phys. **81**, 1773 (2009) [arXiv:0811.1338 [nucl-th]].
 - [14] E. Epelbaum and U.-G. Meißner, Ann. Rev. Nucl. Part. Sci. **62**, 159 (2012) [arXiv:1201.2136 [nucl-th]].
 - [15] R. Machleidt and D. R. Entem, Phys. Rept. **503**, 1 (2011) [arXiv:1105.2919 [nucl-th]].
 - [16] E. Epelbaum, A. Nogga, W. Glöckle, H. Kamada, U.-G. Meißner and H. Witala, Phys. Rev. C **66**, 064001 (2002) [nucl-th/0208023].
 - [17] S. Ishikawa and M. R. Robilotta, Phys. Rev. C **76**, 014006 (2007) [arXiv:0704.0711 [nucl-th]].
 - [18] V. Bernard, E. Epelbaum, H. Krebs and U.-G. Meißner, Phys. Rev. C **77**, 064004 (2008) [arXiv:0712.1967 [nucl-th]].
 - [19] V. Bernard, E. Epelbaum, H. Krebs and U.-G. Meißner, Phys. Rev. C **84**, 054001 (2011) [arXiv:1108.3816 [nucl-th]].
 - [20] H. Witala, J. Golak, R. Skibinski, K. Topolnicki, H. Kamada, E. Epelbaum, W. Glöckle and H. Krebs *et al.*, Few Body Syst. **54**, 897 (2013).
 - [21] J. Golak, R. Skibinski, K. Topolnicki, H. Witala, E. Epelbaum, H. Krebs, H. Kamada and U.-G. Meißner *et al.*, arXiv:1410.0756 [nucl-th].
 - [22] H. Krebs, A. Gasparyan and E. Epelbaum, Phys. Rev. C **85**, 054006 (2012) [arXiv:1203.0067 [nucl-th]].
 - [23] R. Koch, Nucl. Phys. A **448**, 707 (1986).
 - [24] V. Baru, E. Epelbaum, C. Hanhart, M. Hoferichter, A. E. Kudryavtsev and D. R. Phillips, Eur. Phys. J. A **48**, 69 (2012) [arXiv:1202.0208 [nucl-th]].
 - [25] A. Gezerlis, I. Tews, E. Epelbaum, S. Gandolfi, K. Hebeler, A. Nogga and A. Schwenk, Phys. Rev. Lett. **111**, no. 3, 032501 (2013) [arXiv:1303.6243 [nucl-th]].
 - [26] A. Gezerlis, I. Tews, E. Epelbaum, M. Freunek, S. Gandolfi, K. Hebeler, A. Nogga and A. Schwenk, arXiv:1406.0454 [nucl-th].
 - [27] E. Epelbaum, W. Glöckle and U.-G. Meißner, Eur. Phys. J. A **19**, 125 (2004) [nucl-th/0304037].
 - [28] C. Ordonez, L. Ray and U. van Kolck, Phys. Rev. Lett. **72**, 1982 (1994).
 - [29] N. Kaiser, S. Gerstendorfer and W. Weise, Nucl. Phys. A **637**, 395 (1998) [nucl-th/9802071].
 - [30] H. Krebs, E. Epelbaum and U.-G. Meißner, Eur. Phys. J. A **32**, 127 (2007) [nucl-th/0703087].

- [31] E. Epelbaum, H. Krebs and U.-G. Meißner, Nucl. Phys. A **806**, 65 (2008) [arXiv:0712.1969 [nucl-th]].
- [32] E. Epelbaum, H. Krebs and U.-G. Meißner, Phys. Rev. C **77**, 034006 (2008) [arXiv:0801.1299 [nucl-th]].
- [33] G. 't Hooft, Nucl. Phys. B **72**, 461 (1974).
- [34] E. Witten, Nucl. Phys. B **160**, 57 (1979).
- [35] E. E. Jenkins, Ann. Rev. Nucl. Part. Sci. **48**, 81 (1998) [hep-ph/9803349].
- [36] D. B. Kaplan and M. J. Savage, Phys. Lett. B **365**, 244 (1996) [hep-ph/9509371].
- [37] D. B. Kaplan and A. V. Manohar, Phys. Rev. C **56**, 76 (1997) [nucl-th/9612021].
- [38] J. Fujita and H. Miyazawa, Prog. Theor. Phys. **17**, 360 (1957).
- [39] V. Bernard, N. Kaiser and U.-G. Meißner, Nucl. Phys. A **615**, 483 (1997) [hep-ph/9611253].
- [40] E. E. Jenkins, Phys. Rev. D **53**, 2625 (1996) [hep-ph/9509433].
- [41] R. Flores-Mendieta, C. P. Hofmann, E. E. Jenkins and A. V. Manohar, Phys. Rev. D **62**, 034001 (2000) [hep-ph/0001218].
- [42] A. C. Cordon and J. L. Goity, Phys. Rev. D **87**, 016019 (2013) [arXiv:1210.2364 [nucl-th]].
- [43] M. K. Banerjee, T. D. Cohen and B. A. Gelman, Phys. Rev. C **65**, 034011 (2002) [hep-ph/0109274].
- [44] A. V. Belitsky and T. D. Cohen, Phys. Rev. C **65**, 064008 (2002) [hep-ph/0202153].
- [45] T. D. Cohen, Phys. Rev. C **66**, 064003 (2002) [nucl-th/0209072].
- [46] E. Epelbaum, W. Glöckle and U.-G. Meißner, Nucl. Phys. A **637**, 107 (1998) [nucl-th/9801064].
- [47] E. Epelbaum, W. Glöckle and U.-G. Meißner, Nucl. Phys. A **671**, 295 (2000) [nucl-th/9910064].
- [48] L. Girlanda, A. Kievsky and M. Viviani, Phys. Rev. C **84**, 014001 (2011) [arXiv:1102.4799 [nucl-th]].
- [49] J. Golak, D. Rozpedzik, R. Skibinski, K. Topolnicki, H. Witala, W. Glöckle, A. Nogga and E. Epelbaum *et al.*, Eur. Phys. J. A **43**, 241 (2010) [arXiv:0911.4173 [nucl-th]].